Supplement of Geosci. Model Dev., 19, 7217–7237, 2026
https://doi.org/10.5194/gmd-19-7217-2026-supplement

Geoscientific Model Development
Open Access

Supplement of

Resolving effects of leaf pigmentation changes and plant residue on the energy balance of winter wheat cultivation in the ORCHIDEE-CROP model

Ke Yu et al.

Correspondence to: Ke Yu (ke.yu@lsce.ipsl.fr) and Yang Su (yang.su@ens.fr)

S1.1 Quality filtering and preprocessing of surface albedo data at ICOS sites

Surface albedo estimates were derived after a multi-step quality filtering procedure adapted from Cescatti et al. (2012). Half-hourly records of incoming and reflected shortwave radiation (*SW_IN* and *SW_OUT*) were selected only when measurements were available or gap-filled and marked as reliable according to the corresponding quality control (QC) flag (values of 0, 1 and 2; Pastorello et al., 2020). We further required *SW_IN* to exceed 20 W m^{-2} and discarded cases where *SW_OUT* was equal to or greater than *SW_IN*.

To limit contamination from clouds, aerosols, and snow, we applied additional screening based on MODIS ancillary products (MCD43A2 and MOD(Y)D04_L2, https://ladsweb.modaps.eosdis.nasa.gov/). Daily albedo values were retained only when cloud cover remained below 60%, aerosol loading below 40%, and no snow presence was detected. Although applied at a coarse spatial resolution, this screening effectively reduces biases associated with periods of very weak shortwave radiation, for which albedo retrievals are inherently uncertain.

As a final step, we removed extreme values identified as exceeding five standard deviations from the distribution computed over the full analysis period, which predominantly captures residual measurement artifacts and uncharacterized sensor errors.

S1.2 Site-specific degradation of surface albedo simulations

While the modified ORCHIDEE-CROP configuration (ORC-AE) improves the simulation of surface albedo at most sites, degraded performance is observed for two site-years (DE-Geb in 2014 and FR-Aur in 2019). For these site-years, ORC-AE simulates an increase in surface albedo during the foliar yellowing and residue covering periods, whereas the albedo derived from shortwave radiation measurements remains comparatively low (Fig. S5a,c).

To investigate the origin of this mismatch, we examined photographs taken on site around key phenological stages, including the dates of maximum leaf area index (*LAI*), crop maturity, and harvest. These images show visibly bright surface conditions during both foliar yellowing and residue covering periods, possibly associated with high surface reflectivity (Fig. S16). This qualitative evidence suggests that the model captures the expected surface state during these periods at the field scale.

The persistent low albedo values derived from radiometer observations at these two sites may therefore reflect limitations in observational representativeness rather than deficiencies in the model formulation. Radiometer measurements sample a limited spatial footprint, typically on the order of 8-1000 m^2 (Eichler, 2022), and may therefore be influenced by local heterogeneity in residue distribution, sensor viewing geometry, or the partial sampling of surface patches that are not representative of the surrounding field. Such effects are particularly relevant during post-harvest periods, when residue cover can be highly heterogeneous at small spatial scales.

These cases highlight the challenges of evaluating field-scale albedo dynamics using point-scale observations and underscore the importance of combining local measurements with spatially distributed remote sensing data when assessing crop albedo processes.

Supplementary figures

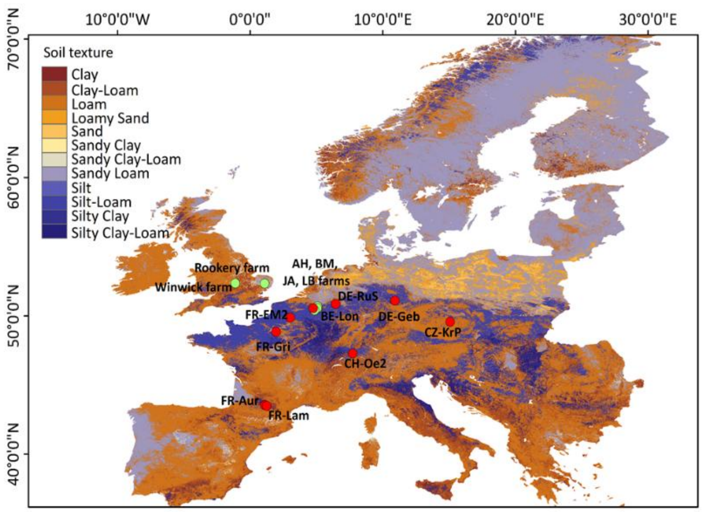

Figure S1 Distribution of the 10 European cropland sites used in the analysis. Data is obtained from two eddy covariance datasets (ICOS (red) and ClieNFarm project (green)). The background data is a 0.01° soil texture map from the USDA.

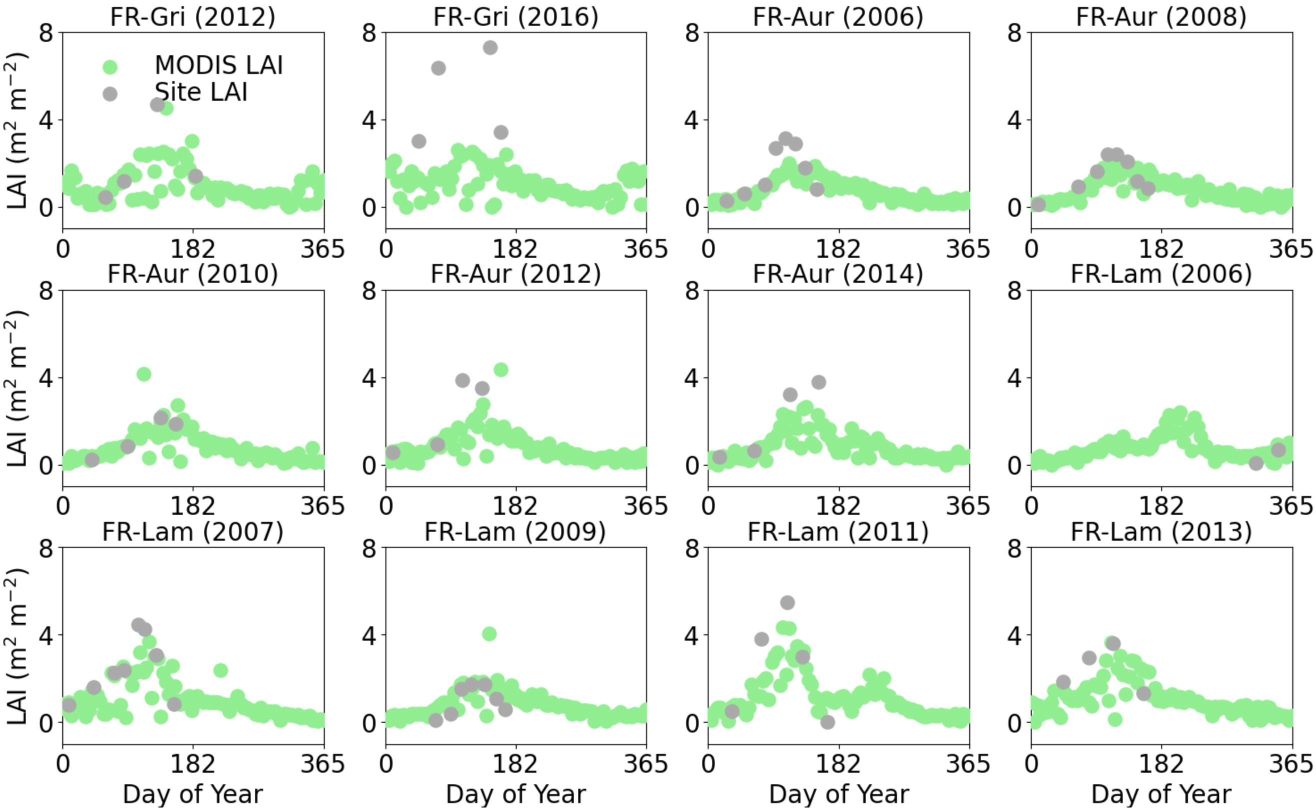

Figure S2 Comparison of leaf area index (*LAI*) between daily satellite-based product (4-day, 500-m MCD15A3H) (green dots) and site measurements (grey dots) at three ICOS sites in different years.

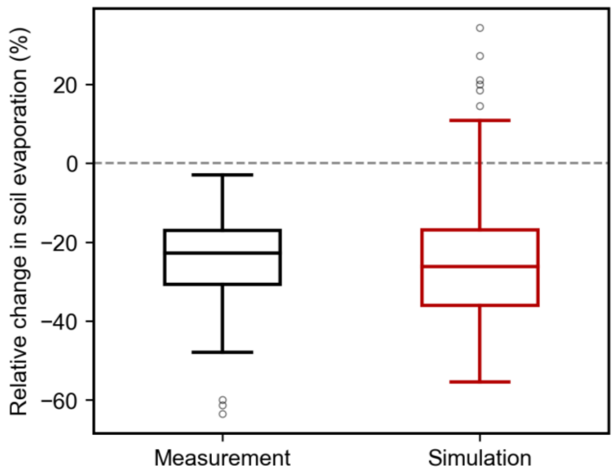

Figure S3. The comparison of relative change in soil evaporation (%) between model simulation and eight field experiments during residue covering periods. Values from model simulation derive from ORC-AE and ORC-D. ORC-AE adjusts surface albedo, soil conductance and surface roughness together in the ORCHIDEE-CROP model. ORC-D is the initial model version. The solid black and red lines within each box indicate the mean values, respectively. The box spans the interquartile range, covering the 25th percentile (lower bound) to the 75th percentile (upper bound). Black crossbars at the top and bottom represent the dataset's minimum and maximum values. The gray hollow circles are outliers. The gray horizontal dotted line represents zero on the y-axis.

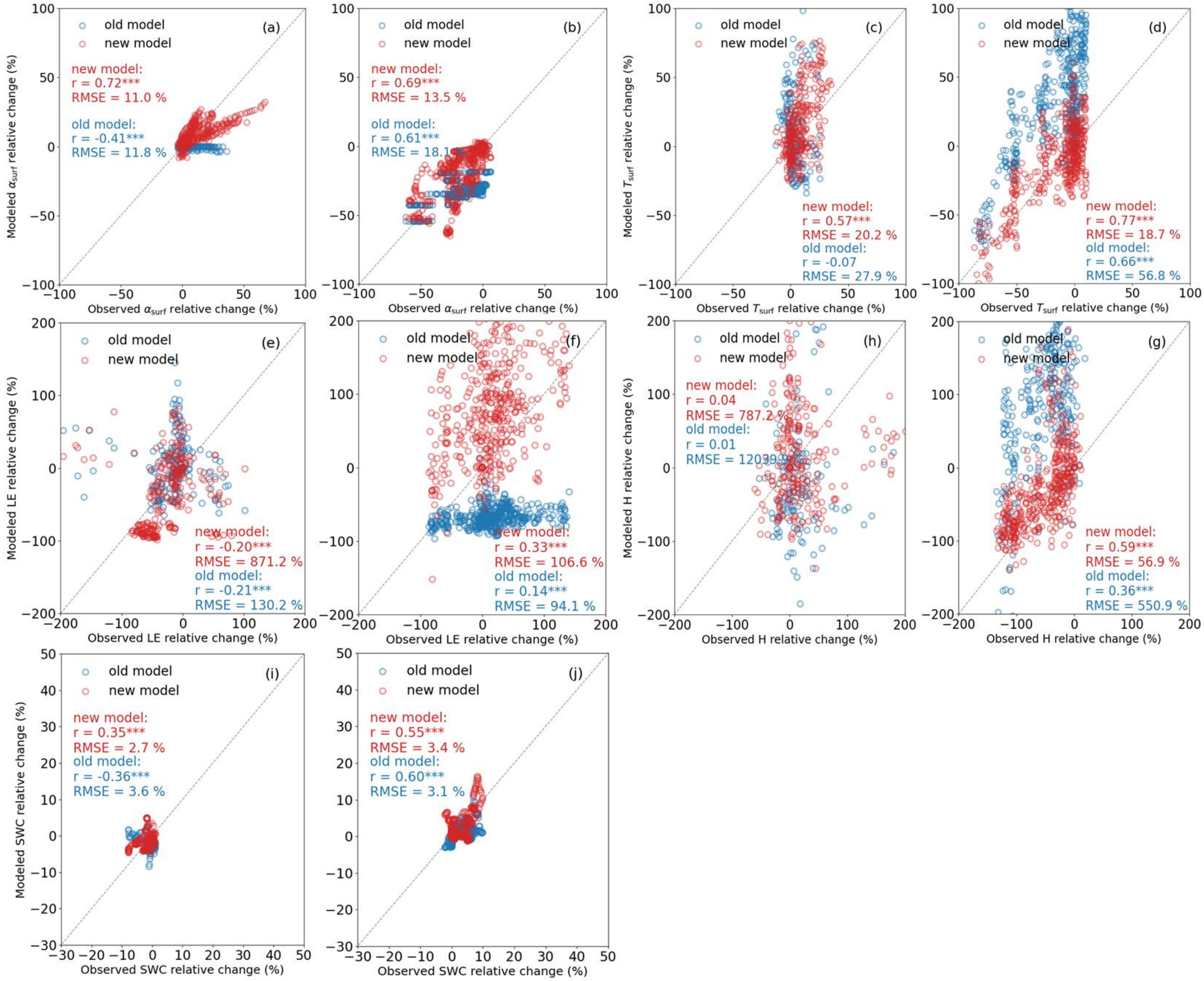

Figure S4. Daily relative changes (normalized to the first day of each period, %) in surface albedo (α_{surf}), surface temperature (T_{surf}), latent (*LE*) and sensible (*H*) heat fluxes, and total soil water content (*SWC*) during the foliar yellowing and residue covering periods across all available sites. The y-axis shows relative changes simulated by ORC-AE (red dots) and ORC-D (blue dots), while the x-axis shows the corresponding relative changes derived from site observations. ORC-AE represents the new model version with effects of the modified α_{surf} and the refined soil conductance (β_4) and surface roughness (Z_0), while ORC-D suggests the initial version of the model. The values of r and RMSE shown in the legend denote the Pearson correlation coefficient and the root mean square error, respectively. '***' shows the comparison passes the significance level of 0.01. The gray dotted line indicates the 1:1 relationship.

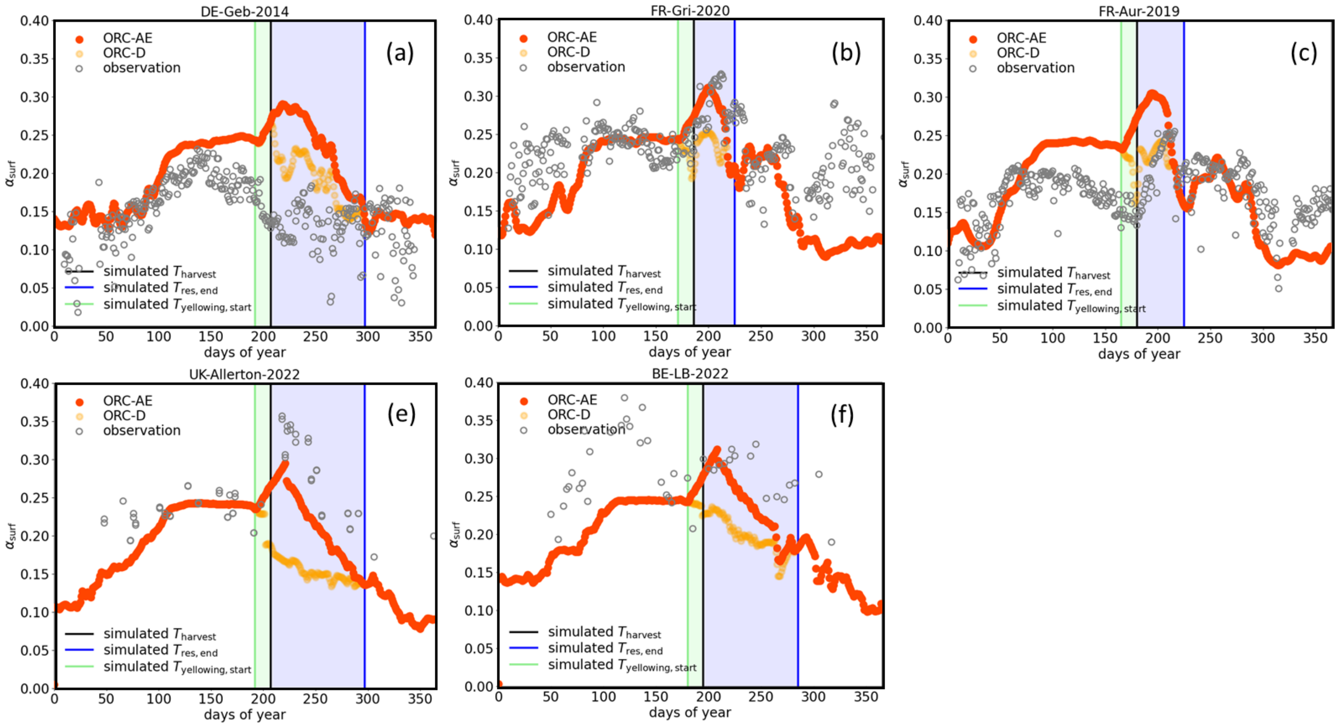

Figure S5 The comparison of surface albedo (α_{surf}) predicted from the old (orange dots, ORC-D) and new (red dots, ORC-AE) ORCHIDEE-CROP models and observations (gray dots) at five test sites in Europe. The observed α_{surf} in (a), (b) and (c) is derived from site radiation measurements through the Integrated Carbon Observation System (ICOS) Data Portal, while α_{surf} observation in (d) and (e) is derived from 5-day 300-m Sentinel-2 α_{surf} product (Lin et al., 2023). The green, black and blue solid lines are the simulated start of the foliar yellowing period (shallow-green area) ($T_{yellowing,\ start}$), harvesting date ($T_{harvest}$) and the end of residue covering period (shallow-blue area) ($T_{res,\ end}$), respectively.

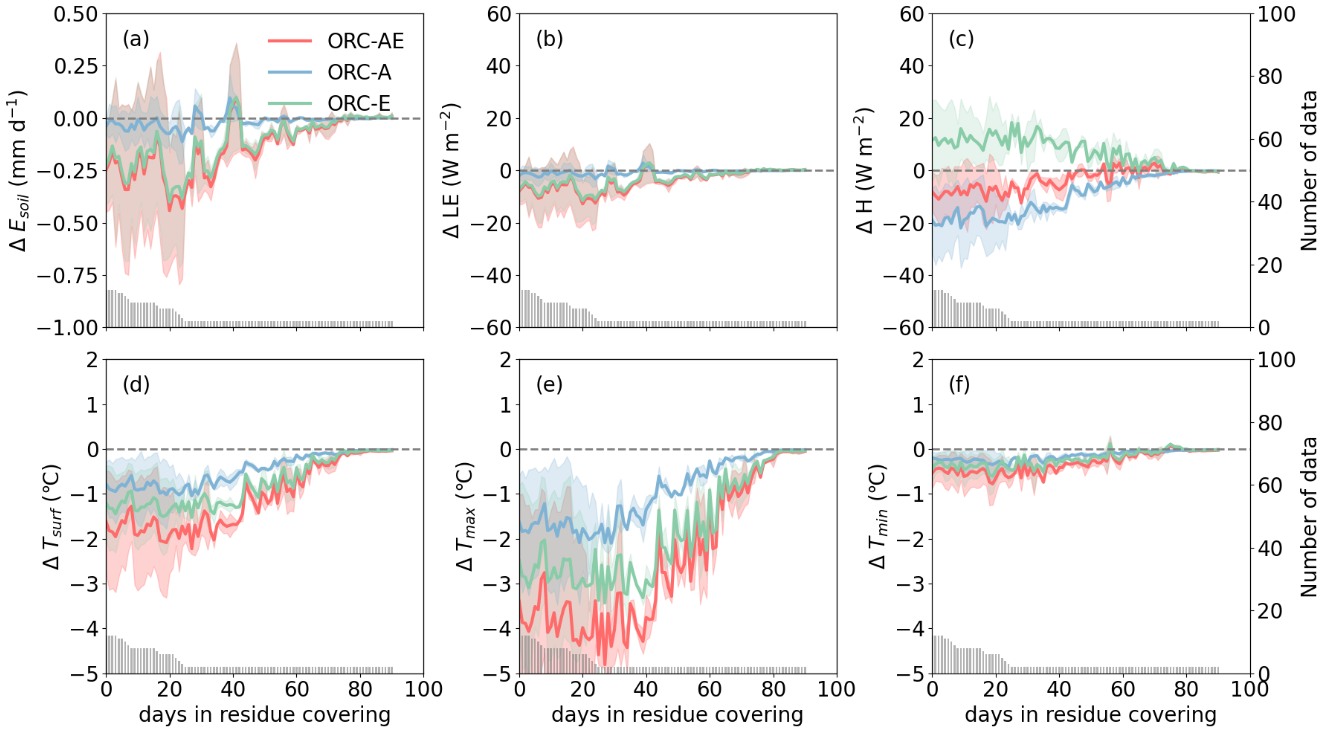

Figure S6 Daily changes of soil evaporation (E_{soil}), surface temperature (T_{surf}), latent and sensible heat fluxes (*LE* and *H*), maximum and minimum surface temperature (T_{max} and T_{min}) from the initial version in ORC-A (blue line), ORC-E (green line), ORC-AE (orange line) experiments in 90 days during residue covering periods across twelve sites. ORC-A represents the modified surface albedo (α_{surf}) in the ORCHIDEE-CROP model. In ORC-E, both the soil conductance (β_4) and surface roughness (Z_0) were adjusted in the ORCHIDEE-CROP model. ORC-AE extends these modifications by adjusting α_{surf}, β_4 and Z_0 together in the ORCHIDEE-CROP model. Areas in different colors represent the standard deviation of variables across all sites in each experiment. The grey dotted vertical line in each plot represents zero on the y-axis. Gray bars on the right y-axis indicate the number of data points per site.

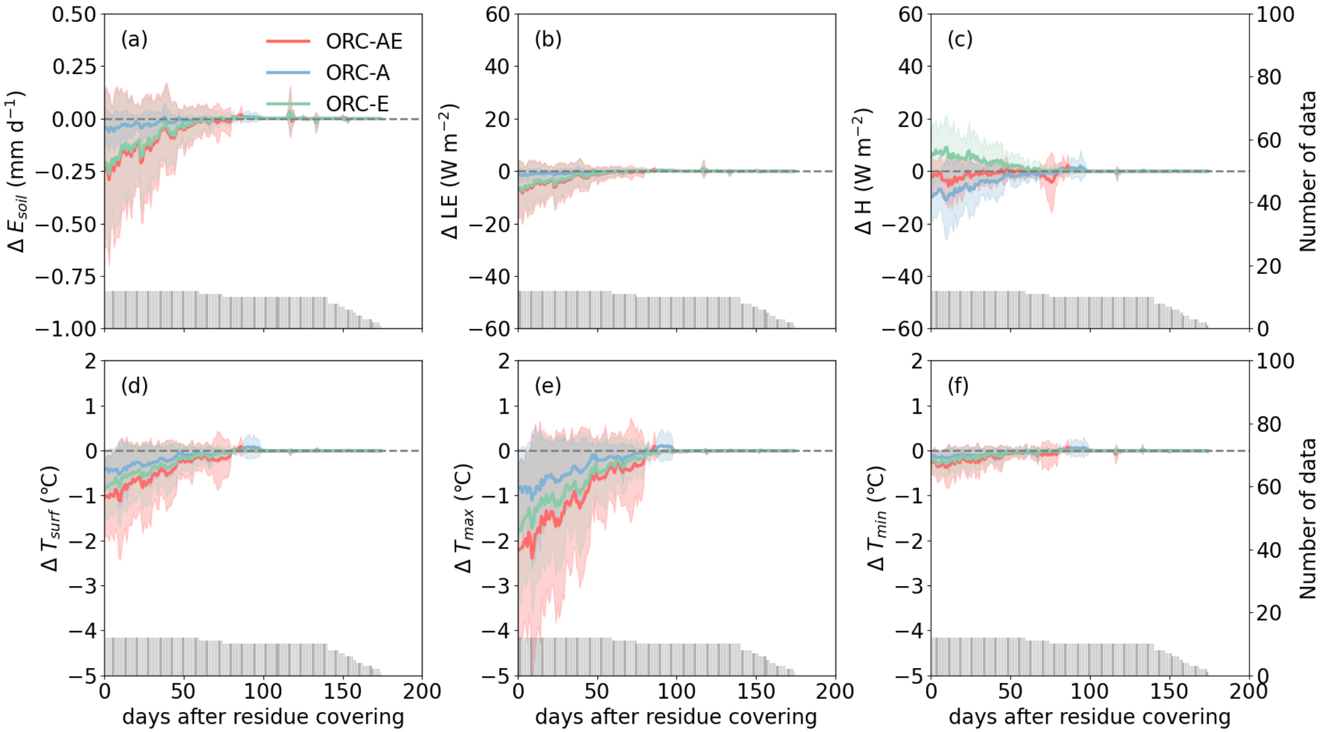

Figure S7 Daily changes of soil evaporation (E_{soil}), surface temperature (T_{surf}), latent and sensible heat fluxes (*LE* and *H*), maximum and minimum surface temperature (T_{max} and T_{min}) from the old model in ORC-A (blue line), ORC-E (green line), ORC-AE (orange line) experiments in days after residue covering periods in the harvest years across 12 sites. ORC-A represents the modified surface albedo (α_{surf}) in the ORCHIDEE-CROP model. In ORC-E, both the soil conductance (β_4) and surface roughness (Z_0) were adjusted in the ORCHIDEE-CROP model. ORC-AE extends these modifications by adjusting α_{surf}, β_4 and Z_0 together in the ORCHIDEE-CROP model. Areas in different colors represent the standard deviation of variables across all sites in each experiment. The grey dotted vertical line in each plot represents zero on the y-axis. Gray bars on the right y-axis indicate the number of data points per site.

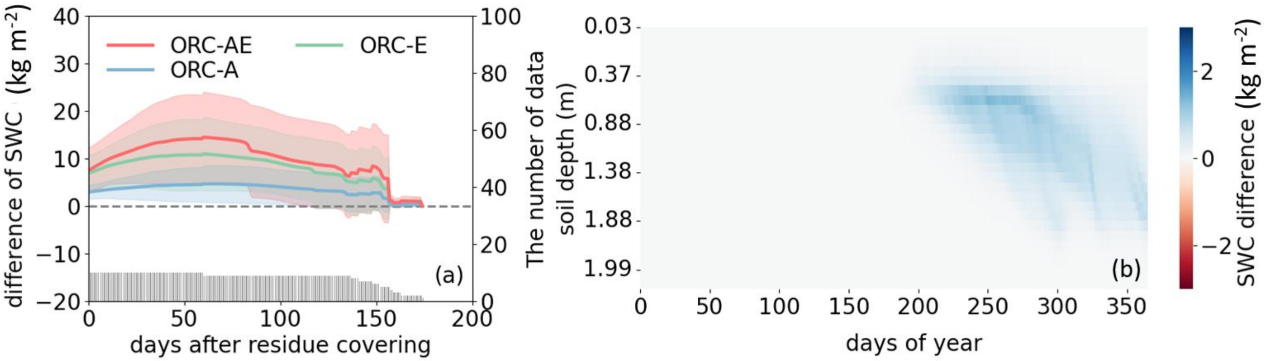

Figure S8 (a) Daily changes of total soil water content (*SWC*) in ORC-A (blue line), ORC-E (green line), ORC-AE experiments (orange line) compared with the initial version in days after residue covering periods in the harvest years across 12 sites. ORC-A represents the modified surface albedo (α_{surf}) in the ORCHIDEE-CROP model. In ORC-E, both the soil conductance (β_4) and surface roughness (Z_0) were adjusted in the ORCHIDEE-CROP model. ORC-AE extends these modifications by adjusting α_{surf}, β_4 and Z_0 together in the ORCHIDEE-CROP model. Areas in different colors represent ranges of standard deviation of *SWC* across all sites. The grey dotted vertical line in each plot represents zero on the y-axis. The gray bars on the right y-axis indicate the number of data points per day. (b) Daily changes of *SWC* in different soil layers up to 2 m in ORC-AE compared to the initial version in the harvest years on average across twelve sites.

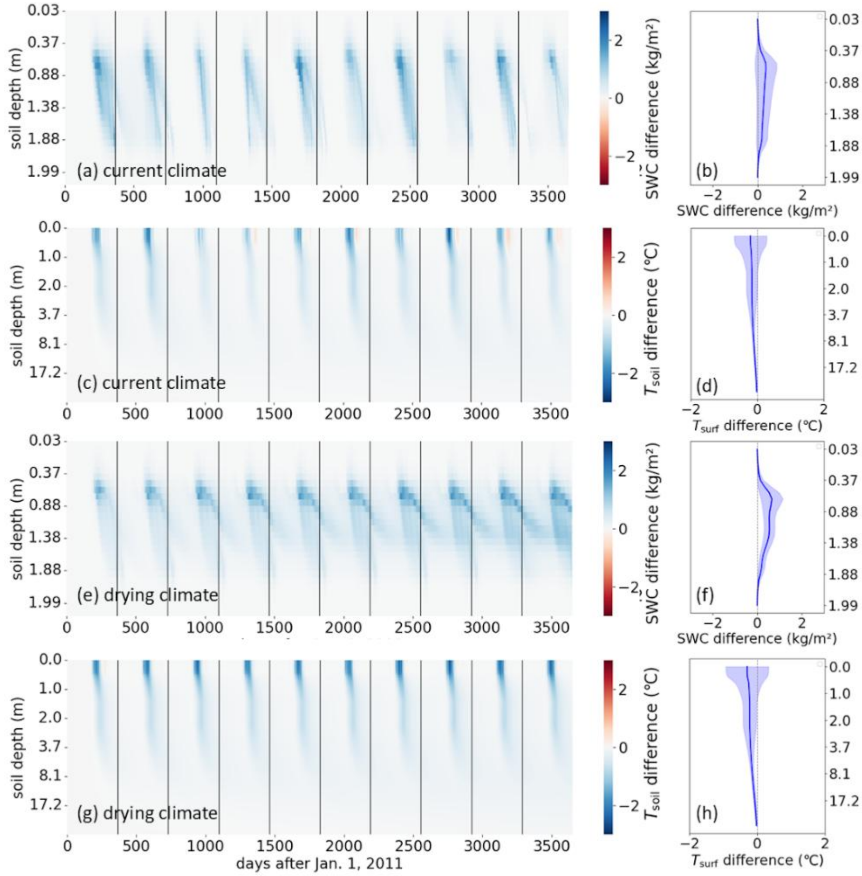

Figure S9 Simulation of soil water content (*SWC*) and soil temperature (T_{soil}) differences between the new (ORC-AE) and the initial version (ORC-D) for winter wheat over a 10-year period (2010-2020) at six sites. ORC-AE adjusts surface albedo (α_{surf}), soil conductance (β_4) and surface roughness (Z_0) together in the ORCHIDEE-CROP model. Shows are only from the year of 2011 and residue cover persists for 60 days post-harvest each year. The *SWC* is within 2 m depths with 27 soil layers while T_{soil} is within 10 m with 90 soil layers. (a)-(d) represent the current scenarios using climate forcing data from the Integrated Carbon Observation System (ICOS) Data Portal. While (e)-(h) shows drying scenarios using ICOS climate forcing data for the year with minimal annual rainfall. (a) and (e) show *SWC* differences by soil depth, with yearly averages at each soil depth shown in (b) and (f). (c) and (g) show T_{soil} differences by soil depth, with yearly averages at each soil depth in (d) and (h). The blue areas in (b), (d), (f) and (h) represent the standard deviations. The vertical black solid lines in (a), (c), (e) and (g) split years.

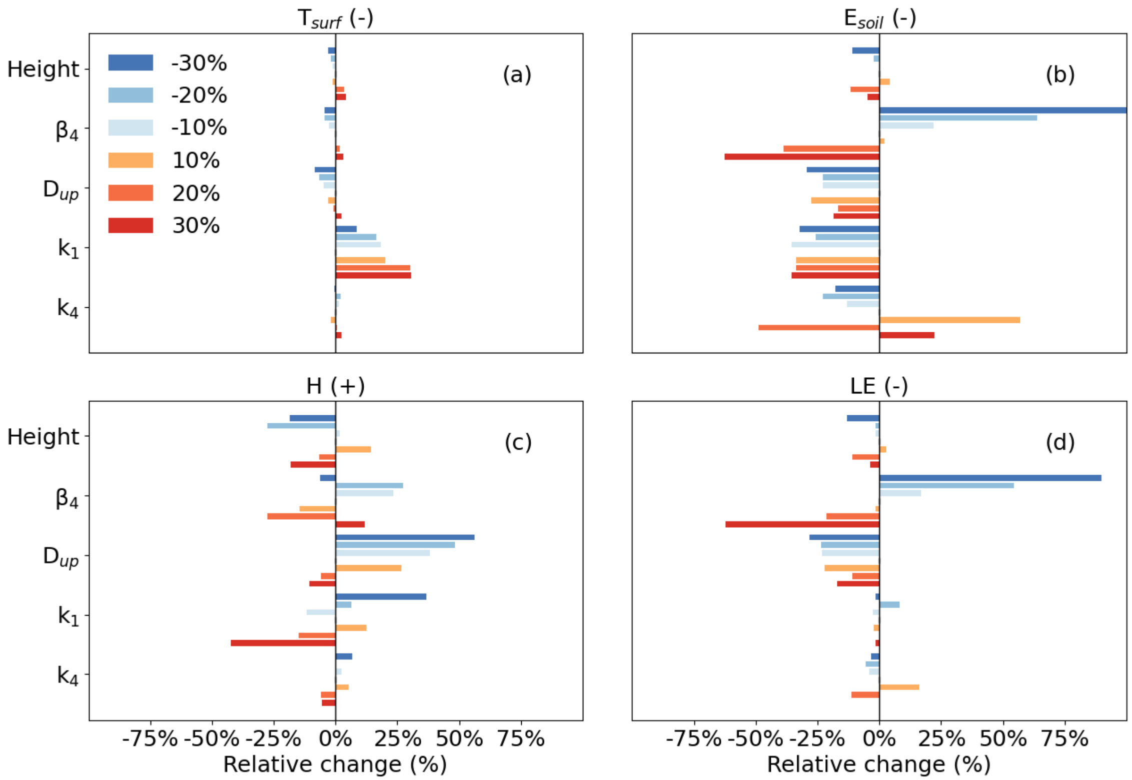

Figure S10 Relative changes in residue impacts on surface temperature (T_{surf}, a), soil evaporation (E_{soil}, b), sensible heat flux (H, c) and latent heat flux (LE, d) by varying ±10, ±20 and ±30% of residue height (Height), soil conductance (β_4), duration of surface albedo increase during residue covering period (D_{up}), slopes (k_1 and k_4) in D_{up} and in surface albedo decrease stages in the modelling. Residue impacts are quantified by relative changes of variables above between ORC-AE and ORC-D. ORC-AE adjusts surface albedo, β_4 and surface roughness together in the ORCHIDEE-CROP model. ORC-D is the initial model version. Parameters are changed one by one, while the others are kept the same. '(+)' and '(-)' behind the subplot titles represent the increase and decrease of variables caused by parameters at baseline condition.

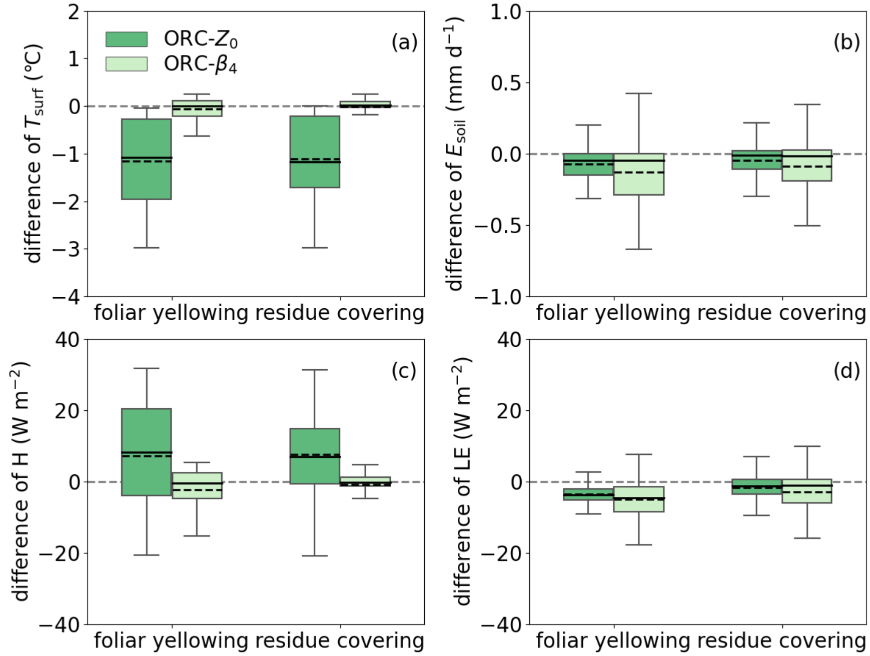

Figure S11 The effect of model refinements on surface temperature (T_{surf}), soil evaporation (E_{soil}), latent and sensible heat fluxes (*LE* and *H*) during foliar yellowing and residue covering periods at 12 sites. Shown are the differences between the new model (ORC-β_4 and ORC-Z_0) and the old model. ORC-Z_0 represents only the surface roughness (Z_0) was modified in the ORCHIDEE-CROP model. ORC-β_4 refers to the modification of the soil conductance (β_4) in the ORCHIDEE-CROP model. The solid and dotted black lines within each box indicate the mean and median values, respectively. The box spans the interquartile range, covering the 25th percentile (lower bound) to the 75th percentile (upper bound). Black crossbars at the top and bottom represent the dataset's minimum and maximum values. The gray horizontal dotted line in each plot represents zero on the y-axis.

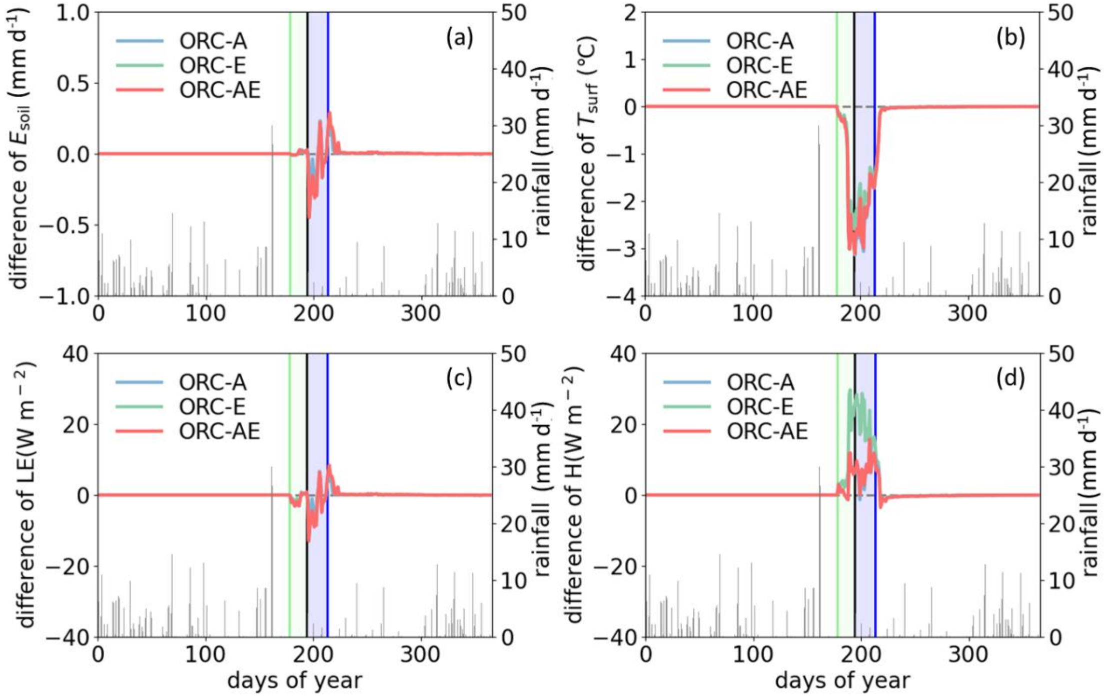

Figure S12 The effect of model refinements on the (a) soil evaporation (E_{soil}), (b) surface temperature (T_{surf}), (c) latent heat flux (*LE*) and (d) sensible heat flux (*H*) among different experiments at the FR-Gri site in 2018. Shown are the differences between the new model and the initial version. ORC-A (blue line) represents the modified surface albedo (α_{surf}) in the ORCHIDEE-CROP model. In ORC-E (green line), both the soil conductance (β_4) and surface roughness (Z_0) were adjusted in the ORCHIDEE-CROP model. ORC-AE (red line) extends these modifications by adjusting α_{surf}, β_4 and Z_0 together in the ORCHIDEE-CROP model. The green, black and blue solid lines are the simulated start of the foliar yellowing period (shallow-green area), harvesting dates and the end of the residue covering period (shallow-blue area), respectively. The grey dotted vertical line in each plot represents zero on the y-axis. The gray bars in the right y-axis are the daily rainfall derived from site observation.

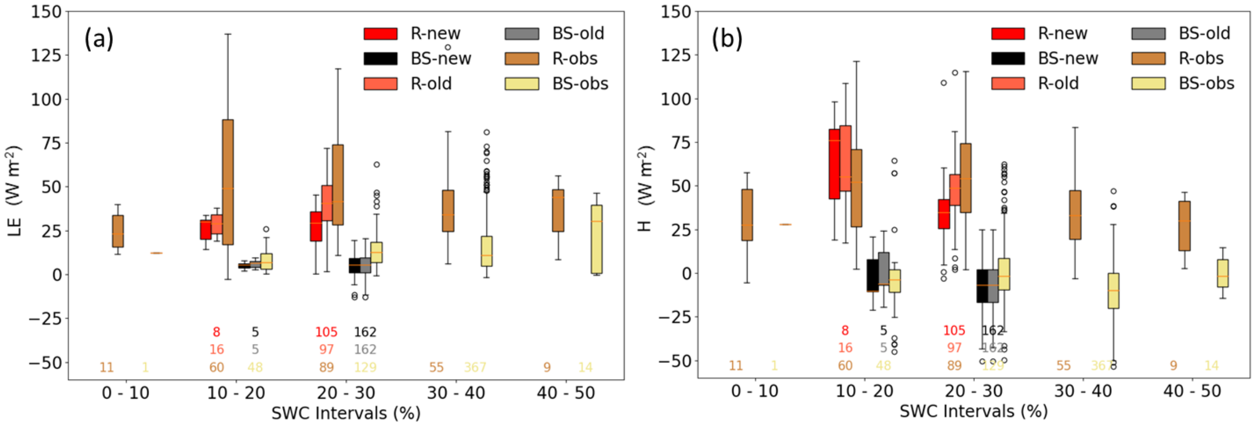

Figure S13 The daily difference of latent and sensible heat flux (*LE* and *H*) between model simulations and observations across different soil water content intervals (*SWC*, %) during residue covering periods and the subsequent bare soil periods at four sites. ORC-AE (R-new and BS-new) adjusts surface albedo (α_{surf}), soil resistance (β_4) and surface roughness (Z_0) together in the ORCHIDEE-CROP model. ORC-D (R-old and BS-old) is the initial version. Observations were obtained from daily eddy-covariance measurements via the Integrated Carbon Observation System (ICOS) Data Portal. The periods of residue covering and bare soil were extracted by identifying site photos. 'R', 'BS' and 'obs' in each plot represent residues, bare soil and observation. Numbers with different colors represent the number of data in each compared dataset. The solid and dotted black lines within each box indicate the mean and median values, respectively. The box spans the interquartile range, covering the 25th percentile (lower bound) to the 75th percentile (upper bound). Black crossbars at the top and bottom represent the dataset's minimum and maximum values. The black hollow circles are outliers. The missing boxes for *SWC* intervals mean no data.

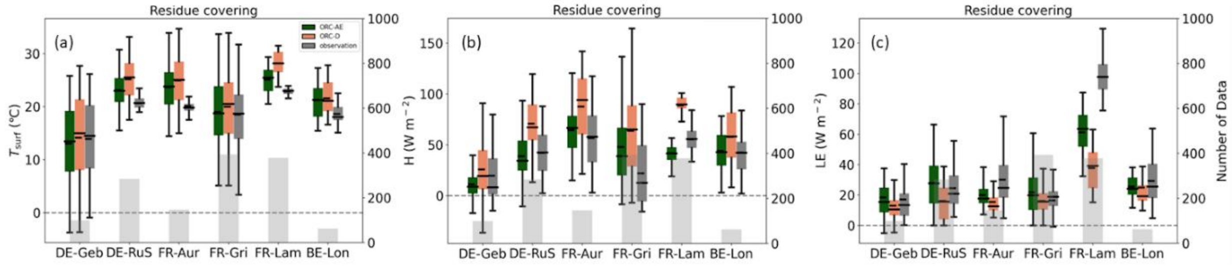

Figure S14 The daily difference of surface temperature (T_{surf}), latent and sensible heat flux (*LE* and *H*) between model simulations and observations during residue covering periods across six sites. ORC-AE (green boxes) adjusts α_{surf}, β_4 and Z_0 together in the ORCHIDEE-CROP model. ORC-D (orange boxes) is the initial version. Observations (gray boxes) were obtained from daily eddy-covariance measurements via the Integrated Carbon Observation System (ICOS) Data Portal. The solid and dotted black lines within each box indicate the mean and median values, respectively. The box spans the interquartile range, covering the 25th percentile (lower bound) to the 75th percentile (upper bound). Black crossbars at the top and bottom represent the dataset's minimum and maximum values. The gray horizontal dotted line in each plot represents zero on the y-axis. The gray bars on the right y-axis show the number of data points per site.

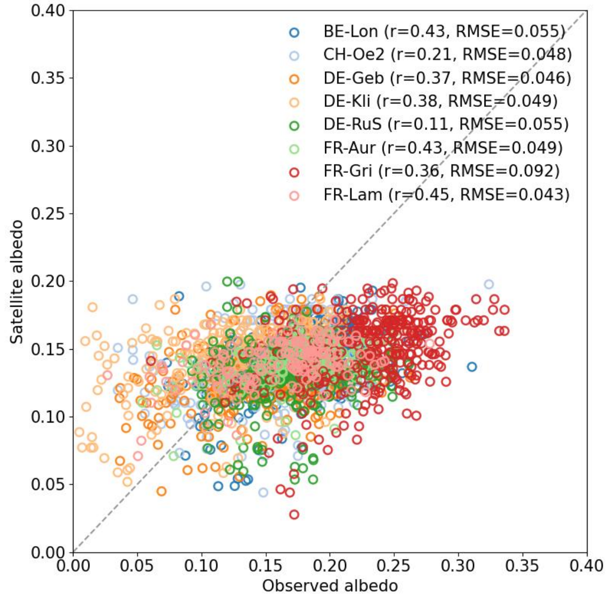

Figure S15 Comparison of surface albedo derived from site measurements (observed albedo) and the 5-day, 300-m Sentinel-2 albedo product (satellite albedo) at eight cropland sites. Site-level surface albedo was calculated as the ratio of outgoing to incoming shortwave radiation. The values of r and RMSE shown in the legend denote the Pearson correlation coefficient and the root mean square error, respectively. The gray dotted line indicates the 1:1 relationship.

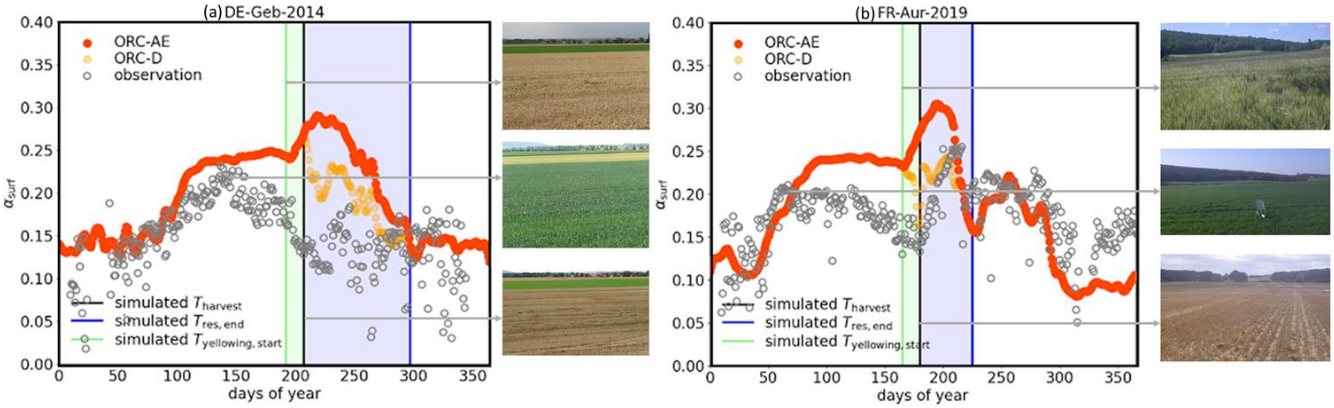

Figure S16 Surface conditions in different winter wheat growing periods at (a) DE-Geb and (b) FR-Aur sites in 2014 and 2019, respectively. Plots represent surface albedo evolutions predicted from the old (orange dots, ORC-D) and new (red dots, ORC-AE) ORCHIDEE-CROP models and observations (gray dots). The observed surface albedo is derived from site radiation measurements through the Integrated Carbon Observation System (ICOS) Data Portal. The green, black and blue solid lines are the simulated start of the foliar yellowing period (shallow-green area), harvesting date and the end of residue covering period (shallow-blue area), respectively. The surface conditions are identified based on site photos obtained from farm managers.

Supplementary Tables

Table S1 Averaged meteorological variables in the year with the lowest annual rainfall at all sites for the drying climate scenario

Site	Drying year	*Ta* (°C)	*Pa* (Pa)	*VPD* (hPa)	*WS* (mm d^{-1})	Precipitation (mm d^{-1})	*SW_IN* (W m^{-2})	*LW_IN* (W m^{-2})
BE-Lon	2011	13.28±6.43	100.17±0.79	3.49±4.11	3.05±1.48	0.02±0.12	125.78±193.41	319.53±36.08
FR-Aur	2014	13.61±6.36	98.50±0.70	4.41±4.88	3.08±1.95	0.03±0.19	159.52±244.33	334.63±38.39
DE-RuS	2018	11.82±8.13	100.41±0.86	4.93±6.64	1.78±1.23	0.03±0.20	137.92±220.17	323.81±45.38
DE-Geb	2019	10.86±7.99	98.52±0.99	4.81±6.03	3.39±1.81	0.02±0.10	131.28±201.68	306.34±42.24
FR-Lam	2011	14.88±7.33	99.52±0.71	6.67±6.97	3.01±1.66	0.03±0.20	162.22±239.51	327.84±40.41
FR-Gri	2020	12.92±6.64	100.34±0.95	5.37±6.24	3.21±1.62	0.03±0.09	144.72±223.33	348.67±32.57

Table S2 Site information

Site	Sowing	Harvest	Tillage	Calibrated duration between maturity and harvest	Observed annual T_{surf}	Observed annual *SWC*	Annual rainfall	Resource
BE-Lon	2012/10/25	2013/8/12	-	19	10.53	33.98	1.70	ICOS
	2014/10/14	2015/8/2	2015/8/21	23	10.89	31.22	1.74	
	2010/10/14	2011/8/16	-	31	11.56	29.83	1.21	
	2018/10/10	2019/8/1	2019/8/7	21	10.78	28.77	1.92	
CH-Oe2	2018/10/11	2019/7/23	2019/8/9	20	11.54	24.35	3.22	ICOS
DE-Geb	2013/8/12	2014/8/8	-	27	11.37	19.24	1.47	ICOS
	2015/9/29	2016/8/7	-	21	10.56	18.40	1.32	
	2018/10/19	2019/7/24	2019/7/27	25	12.09	14.24	0.96	
DE-Kli	2010/10/2	2011/8/22	-	23	8.83	38.14	2.12	ICOS
	2015/9/18	2016/8/24	2016/9/1	26	8.58	-	2.09	
DE-RuS	2012/10/19	2013/8/11	-	21	9.81	32.42	1.30	ICOS
	2014/10/25	2015/8/2	2015/8/5	27	11.22	26.75	1.42	
	2019/10/26	2020/7/28	-	27	12.22	25.56	1.67	

	2017/10/25	2018/7/16	-	13	11.61	17.19	1.20	
FR-Aur	2011/10/21	2012/7/14	-	17	12.90	21.86	1.51	
	2013/10/26	2014/7/10	-	23	13.77	23.93	1.37	ICOS
	2016/12/2	2017/7/5	2017/8/3	19	13.66	22.82	1.88	
FR-Gri	2015/10/21	2016/7/29	2016/8/9	19	11.17	46.29	1.58	
	2013/10/8	2014/8/5	-	22	9.75	28.19	1.80	ICOS
	2011/10/20	2012/8/3	-	23	11.38	28.50	1.70	
FR-Lam	2010/11/3	2011/7/2	-	20	14.12	34.21	1.29	
	2012/10/29	2013/7/22	-	17	13.57	29.23	2.48	
	2015/10/20	2016/7/20	2016/8/10	20	13.91	24.72	1.65	ICOS
	2017/11/16	2018/7/17	2018/9/25	24	14.71	29.42	2.26	
UK-Rookery	2021/10/15	2022/8/2	-	25	10.16	22.51	1.32	
UK-Winwick	2021/10/13	2022/8/9	-	27	-	-	-	ClieNFarm
UK-Allerton	2021/10/16	2022/8/10	-	22	-	-	-	
BE-AH	2021/10/28	2022/7/28	-	21	9.11	1.44	-	ClieNFarm

BE-BM	2021/11/1	2022/8/1	-	24	11.78	1.40	-
BE-LB	2021/10/18	2022/7/25		22	11.73	1.32	-

'-' represent there is no observation at site

Table S3 Canopy height and *LAI* measurements of winter wheat at ICOS cropland sites

Site	Year	Canopy height averaged during growing season (m)	Maximum canopy height (m)	*LAI* averaged during growing season (-)
BE-Lon	2015	0.68±0.32	0.97	-
DE-Geb	2014	0.49±0.34	0.95	-
	2016	0.28±0.31	0.95	-
FR-Aur	2006	0.38±0.25	0.68	1.64±1.12
	2008	0.51±0.26	0.76	1.44±0.82
	2010	0.51±0.34	0.78	1.27±0.89
	2012	0.41±0.05	0.75	1.75±0.68
	2014	0.55±0.03	0.93	1.59±0.41
	2019	0.60±0.03	1.01	-
FR-Lam	2007	0.51±0.33	0.91	2.18±1.55
	2009	0.44±0.26	0.70	0.90±0.72
	2011	0.56±0.39	0.90	2.57±2.30
	2013	0.57±0.11	1.03	2.42±0.72
FR-Gri	2012	0.46±0.28	0.75	1.94±0.32
	2016	0.48±0.32	1.10	5.02±0.42
	2018	0.43±0.04	0.89	-

2020	0.48±0.05	0.95	-

'-' represent there is no measurement at site

Table S4. Site experiments to analyze changes in soil evaporation due to residue coverage

Residue covering period	Site location	Latitude, Longitude	Relative change (%)	Reference
March-July in 1997-1998	Losses Plateau, China	35°33’N, 104°35’E	-6.05	Huang et al., 2005
May-August in 2012	Chengcheng, China	37.89° N, 114.69° E	-26.14	Li et al., 2013
June-September in 2007-2019	Heyang, China	35°19’N, 110°4’E	-30.09	Li et al., 2022
April-June in 2014	Beijing, China	39°37′N, 116°25′E	-31.31	Wang et al., 2018
June-July in 1999	Luancheng, China	37°53’N, 114°40’E	-61.30	Zhang et al., 2005
October 1988-June 1989	Merredin, Australia	31 °29’S, 118°12’E	-2.98	Yunusa et al., 1994
September-October, December 2008	Londrina, Brazil	23º18’S, 51º09’W	-17.48	Gava et al., 2013
June 2018-September 2018	Ahvaz, Iran	31.30° N, 48.65° E	-22.72	Yusefi et al., 2020
November 2023-January 2024	Henan, China	35°14’N,113°76’E	-18.5	Wang et al., 2025
-	Losses Plateau, China	34°17’N, 108°04’E	-19.46	Xing et al., 2017

June-Septemble 2002-2004	Heyang, China	35°19’37”N, 110°4’57”E	-17.22	Zhang et al., 2016
June-August 2010-2011	Beijing, China	39.6° N, 116.8° E	-21.67	Li et al., 2015

Table S5 Relative changes of soil evaporation (E_{soil}), surface temperature (mean (T_{surf}), max (T_{max}) and min (T_{min})), latent heat flux (LE), sensible heat flux (H) and soil water content (SWC) induced by modifications in surface albedo (α_{surf}), surface roughness (Z_0), and soil conductance (β_4) in ORC-AE, ORC-A, and ORC-E during foliar yellowing and residue covering periods, compared with the standard version of ORCHIDEE-CROP (ORC-D).

		E_{soil} (mm d^{-1})	T_{surf} (°C)	T_{max} (°C)	T_{min} (°C)	LE (W m^{-2})	H (W m^{-2})	SWC (kg m^{-2})
ORC-AE	Foliar yellowing	**-0.18±0.08 (-16.85±13.23%)**	**-1.55±0.93 (-6.01±3.03%)**	**-3.33±2.02 (-9.20±4.52%)**	**-0.38±0.22 (-2.23±1.20%)**	**-6.84±1.41 (-20.24±12.35%)**	**-8.10±4.18 (-18.78±9.66%)**	5.13±3.90 (20.53±55.49%)
	Residue covering	**-0.17±0.14 (-3.56±32.15%)**	**-1.90±0.88 (-7.41±2.17%)**	**-4.11±1.84 (-11.21±3.14%)**	**-0.56±0.28 (-3.31±1.06%)**	**-5.15±4.03 (-3.61±32.23%)**	**-7.44±3.98 (-8.97±8.43%)**	13.30±8.02 (22.48±54.01%)
ORC-A	Foliar yellowing	-0.02±0.02 (-0.24±3.94%)	**-0.71±0.37 (-2.81±1.17%)**	**-1.47±0.78 (-4.21±1.66%)**	**-0.16±0.09 (-0.94±0.50%)**	**-2.17±1.67 (-3.76±3.96%)**	**-17.01±7.78 (-27.22±7.84%)**	1.90±3.67 (3.60±8.81%)
	Residue covering	**-0.03±0.02 (-1.83±4.52%)**	**-0.82±0.33 (-3.24±0.95%)**	**-1.70±0.66 (-4.68±1.27%)**	**-0.24±0.11 (-1.47±0.58%)**	**-1.28±0.92 (-2.00±4.84%)**	**-17.24±5.72 (-21.22±7.29%)**	3.38±6.20 (2.23±6.08%)
ORC-E	Foliar yellowing	**-0.19±0.10* (-17.60±11.90%)**	**-1.17±0.62 (-4.58±2.03%)**	**-2.53±1.38 (-7.08±3.07%)**	**-0.30±0.15 (-1.78 0.81%)**	**-6.85±1.80 (-21.11±9.51%)**	9.37±9.60 (0.52±15.48%)	4.85±2.57 (0.98±0.69%)
	Residue covering	**-0.19±0.09 (-8.36±17.48%)**	**-1.38±0.63 (-5.42±1.55%)**	**-2.99±1.25 (-8.25±2.14%)**	**-0.42±0.23 (-2.47±0.89%)**	**-5.59±2.70 (-8.37±17.54%)**	**12.47±6.37 (14.00±7.27%)**	**12.09±8.04(1.78±0.70%)**

Bold values indicate a significant t-test ($p<0.05$). The value in brackets indicates the relative change.

Reference

Cescatti, A., Marcolla, B., Santhana Vannan, S. K., Pan, J. Y., Román, M. O., Yang, X., Ciais, P., Cook, R. B., Law, B. E., Matteucci, G., Migliavacca, M., Moors, E., Richardson, A. D., Seufert, G., and Schaaf, C. B.: Intercomparison of MODIS albedo retrievals and in situ measurements across the global FLUXNET network, Remote Sens. Environ., 121, 323-334, https://doi.org/10.1016/j.rse.2012.02.019, 2012.

Eichler, S. E.: Portable apparatus for high spatial and temporal resolution of in situ real-time surface albedo measurement in agricultural fields, Environ. Sci. Adv., 1, 297-304, https://doi-org.insu.bib.cnrs.fr/10.1039/d1va00051a, 2022.

Gava, R., de Freitas, P. S. L., de Faria, R. T., Rezende, R., and Frizzone, J. A.: Soil water evaporation under densities of coverage with vegetable residue, Eng. Agric., 33, 116-127, https://doi.org/10.1590/S0100-69162013000100010, 2013.

Huang, Y., Chen, L., Fu, B., Huang, Z., and Gong, J.: The wheat yields and water-use efficiency in the Loess Plateau: straw mulch and irrigation effects, Agric. Water Manage., 72, 209–222, https://doi.org/10.1016/j.agwat.2004.09.012, 2005.

Pastorello, G., Trotta, C., Canfora, E., et al.: The FLUXNET2015 dataset and the ONEFlux processing pipeline for eddy covariance data, Sci. Data, 7, 225, https://doi.org/10.1038/s41597-020-0534-3, 2020.

Li, S. X., Wang, Z. H., Li, S. Q., Gao, Y. J., and Tian, X. H.: Effect of plastic sheet mulch, wheat straw mulch, and maize growth on water loss by evaporation in dryland areas of China, Agric. Water Manage., 116, 39–49, https://doi.org/10.1016/j.agwat.2012.10.004, 2013.

Li, H., Zhang, Y., Sun, Y., Zhang, Q., Liu, P., Wang, X., Li, J., and Wang, R.: No-tillage with straw mulching improved grain yield by reducing soil water evaporation in the fallow period: A 12-year study on the Loess Plateau, Soil Tillage Res., 224, 105504, https://doi.org/10.1016/j.still.2022.105504, 2022.

Li, Y., Liu, H., and Huang, G.: Modeling resistance of soil evaporation and soil evaporation under straw mulching, T. Chinese Soc. Agric. Eng., 31, 98-106, https://doi.org/10.3969/j.issn.1002-6819.2015.01.015, 2015.

Wang, S., Lei, L., Gao, Y., and Zhan, E.: Effects of Straw Decomposition on Soil Surface Evaporation Resistance and Evaporation Simulation, Plants, 14, 434, https://doi.org/10.3390/plants14030434, 2025.

Wang, J., Zhang, Y., Gong, S., Xu, D., Juan, S., and Zhao, Y.: Evapotranspiration, crop coefficient and yield for drip-irrigated winter wheat with straw mulching in North China Plain, Field Crops Res., 217, 218-228, https://doi.org/10.1016/j.fcr.2017.08.021, 2018.

Xing, X., Li, Y., and Ma, X.: Effects on Infiltration and Evaporation When Adding Rapeseed-Oil Residue or Wheat Straw to a Loam Soil, Water, 9, 700, https://doi.org/10.3390/w9090700, 2017.

Yusefi, A., Farrokhian Firouzi, A., and Aminzadeh, M.: The effects of shallow saline groundwater on evaporation, soil moisture, and temperature distribution in the presence of straw mulch, Hydrol. Res., 51, 720-738, https://doi.org/10.2166/nh.2020.010, 2020.

Yunusa, I. A. M., Sedgley, R. H., and Siddique, K. M. H.: Influence of mulching on the pattern of growth and water use by spring wheat and moisture storage on a fine textured soil, Plant Soil, 160, 119-130, https://doi.org/10.1007/BF00010145, 1994.

Zhang, X., Chen, S., Liu, M., Pei, D. and Sun, H. Improved Water Use Efficiency Associated with Cultivars and Agronomic Management in the North China Plain. Agron. J., 97: 783-790. https://doi-org.insu.bib.cnrs.fr/10.2134/agronj2004.0194, 2005.

Zhang, S., Yang, X., and Lovdahl, L.: Soil Management Practice Effect on Water Balance of a Dryland Soil during Fallow Period on the Loess Plateau of China, Soil Water Res., 11, 64-73, https://doi.org/10.17221/15/2015-SWR, 2016.